Science Signaling
AAAS

www.sciencesignaling.org/cgi/content/full/11/513/eaan6831/DC1

Supplementary Materials for

Inactivating mutations in Drosha mediate vascular abnormalities similar to hereditary hemorrhagic telangiectasia

Xuan Jiang, Whitney L. Wooderchak-Donahue, Jamie McDonald, Prajakta Ghatpande, Mai Baalbaki, Melissa Sandoval, Daniel Hart, Hilary Clay, Shaun Coughlin, Giorgio Lagna, Pinar Bayrak-Toydemir,* Akiko Hata*

*Corresponding author. Email: pinar.bayrak-toydemir@aruplab.com (P.B.-T.); akiko.hata@ucsf.edu (A.H.)

Published 16 January 2018, *Sci. Signal.* **11**, eaan6831 (2018)
DOI: 10.1126/scisignal.aan6831

This PDF file includes:

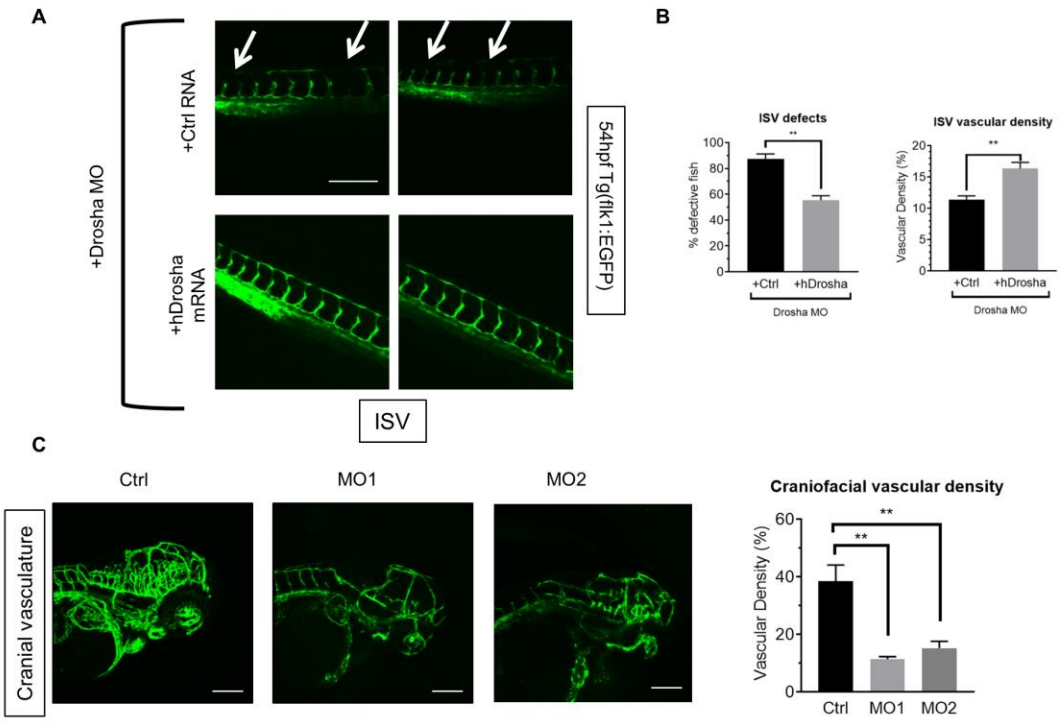

Fig. S1. *Drosha* morphants develop angiogenesis defects. A. *Drosha* MO (1ng MO1+1ng MO2) and 100 pg T7 (Ctrl) RNA or human *Drosha* (*hDrosha*) mRNA were injected into *(flk1:egfp)*^{s843} zebrafish at the 1-2 cell stage. Representative images of ISVs in the middle region of the fish are shown. Arrows: abnormal ISVs. Scale bar: 200µm. **B.** Left: The percentage of embryos with abnormal ISVs was quantitated and shown as Mean±SEM. Right:Quantification of ISV vascular density is shown as Mean±SEM. N=97 zebrafish for Ctrl mRNA and 88 zebrafish for hDrosha mRNA. **P<0.01, significant by two tail unpaired Student t-Test. **C.** Representative Craniofacial images of morpholino-injected fish are shown. Quantification of vascular density is shown as Mean±SEM(right). **P<0.01, significant by one-way ANOVA with post hoc Tukey's test. n=3 zebrafish for Ctrl NO, n=4 zebrafish for MO1 and n=3 zebrafish for MO2. Scale bar: 200 µm.

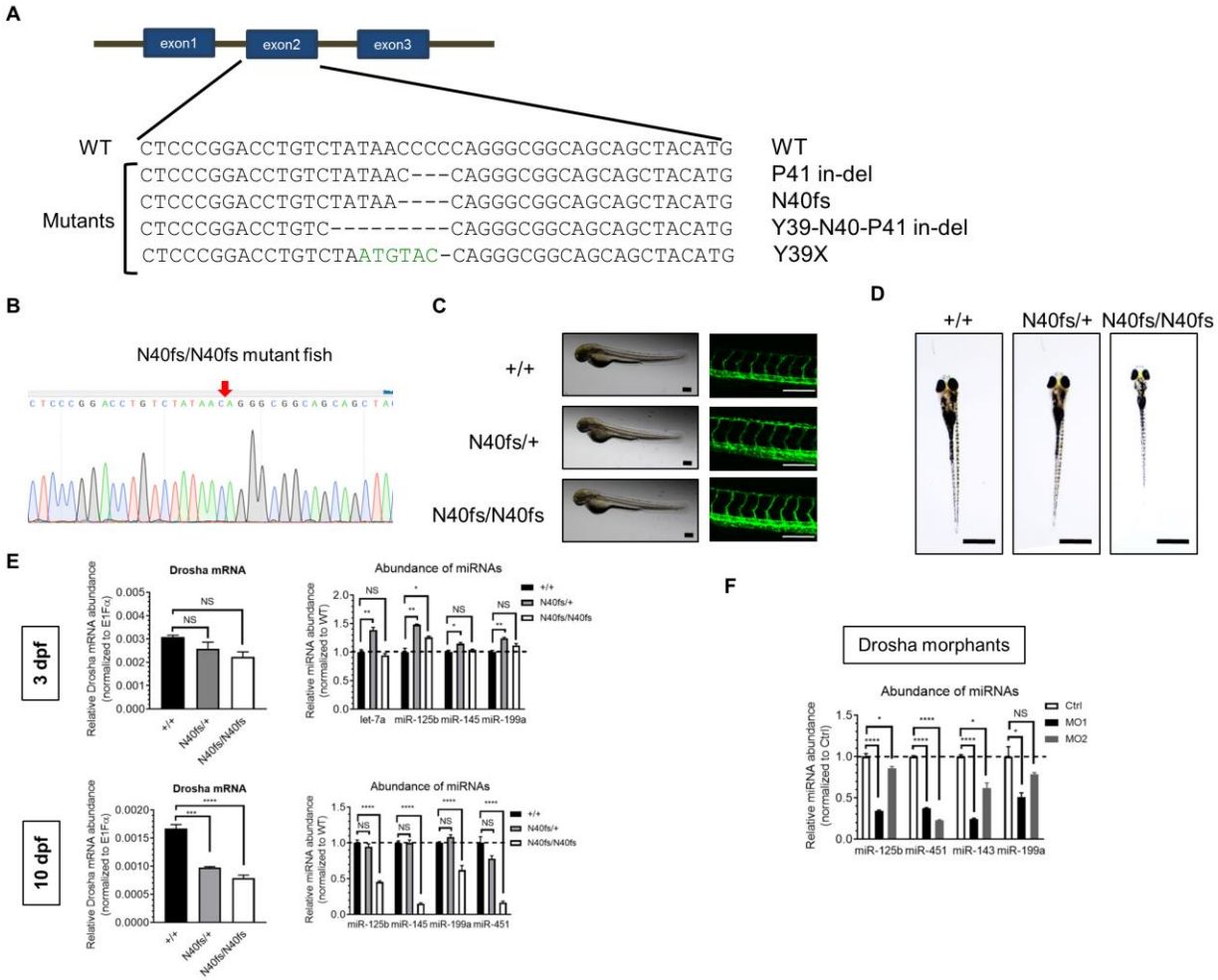

Fig. S2. Generating *Drosha* mutant fish by CRISPR/Cas9. A. CRISPR/Cas9 genome editing technology was applied to introduce mutations in the exon2 of the *Drosha* gene in *Tg(fli1:nEGFP)*^{y7} zebrafish. All insertion or deletion mutants generated by a single CRISPR/Cas9 mutagenesis are shown. **B.** The sequencing result of N40fs/N40fs homozygous mutant is shown. **C.** Representative bright field (left) and fluorescence images (right) of +/+, N40fs/+, or N40fs/N40fs fish at 3 dpf are shown. Scale bar: 200 μm. N=8 zebrafish for each genotype. **D.** Representative bright field images of +/+, N40fs/+, or N40fs/N40fs fish at 10 dpf are shown. Scale bar: 1mm. N=5 zebrafish for each genotype. **E.** The abundance of *Drosha* mRNA normalized to *E1Fα* mRNA (left) and miRNA (right) of +/+, N40fs/+, or N40fs/N40fs fish at 3 dpf (top) and 10 dpf (bottom) was examined by qRT-PCR and shown as Mean ± SEM. Half of the zebrafish was cut off for genotyping, and the other half was frozen for RNA prep and qRT-PCR analysis. N=6 zebrafish for each genotype. **F.** Abundance of miRNAs (miR-125b, -143, -199a, and -451) of *Drosha* morphants (MO1 or MO2) at 3 dpf were examined by qRT-PCR and shown as Mean ± SEM. N=6 zebrafish for each morpholino. In panels E-F, NS indicates not significant; *P<0.05, **P<0.01, ****P<0.0001, significant by one-way ANOVA with post hoc Tukey's test.

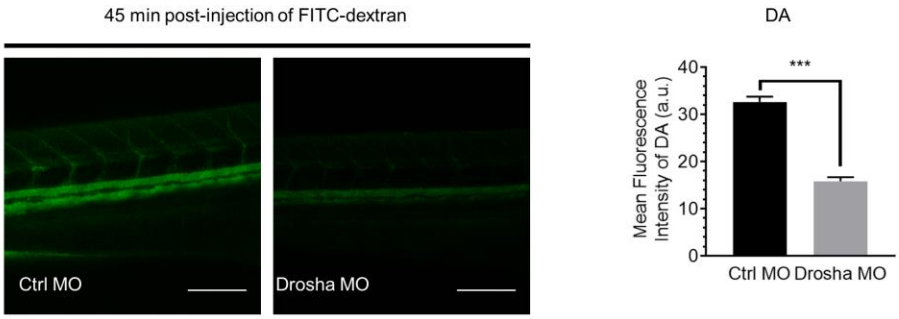

Fig. S3. *Drosha* morphants showed vascular leakiness. Angiography was performed with *Drosha* morphants or Ctrl MO injected fish at 54 hpf. Images were taken 45 min after injection (left). Representative images are shown. Mean fluorescence intensity of dorsal aorta (DA) was quantitated and presented as Mean ±SEM. ***P<0.001, significant by two tail unpaired Student t-Test. Scale bar: 200μm. N=3 zebrafish for each morpholino. a.u. arbitrary units.

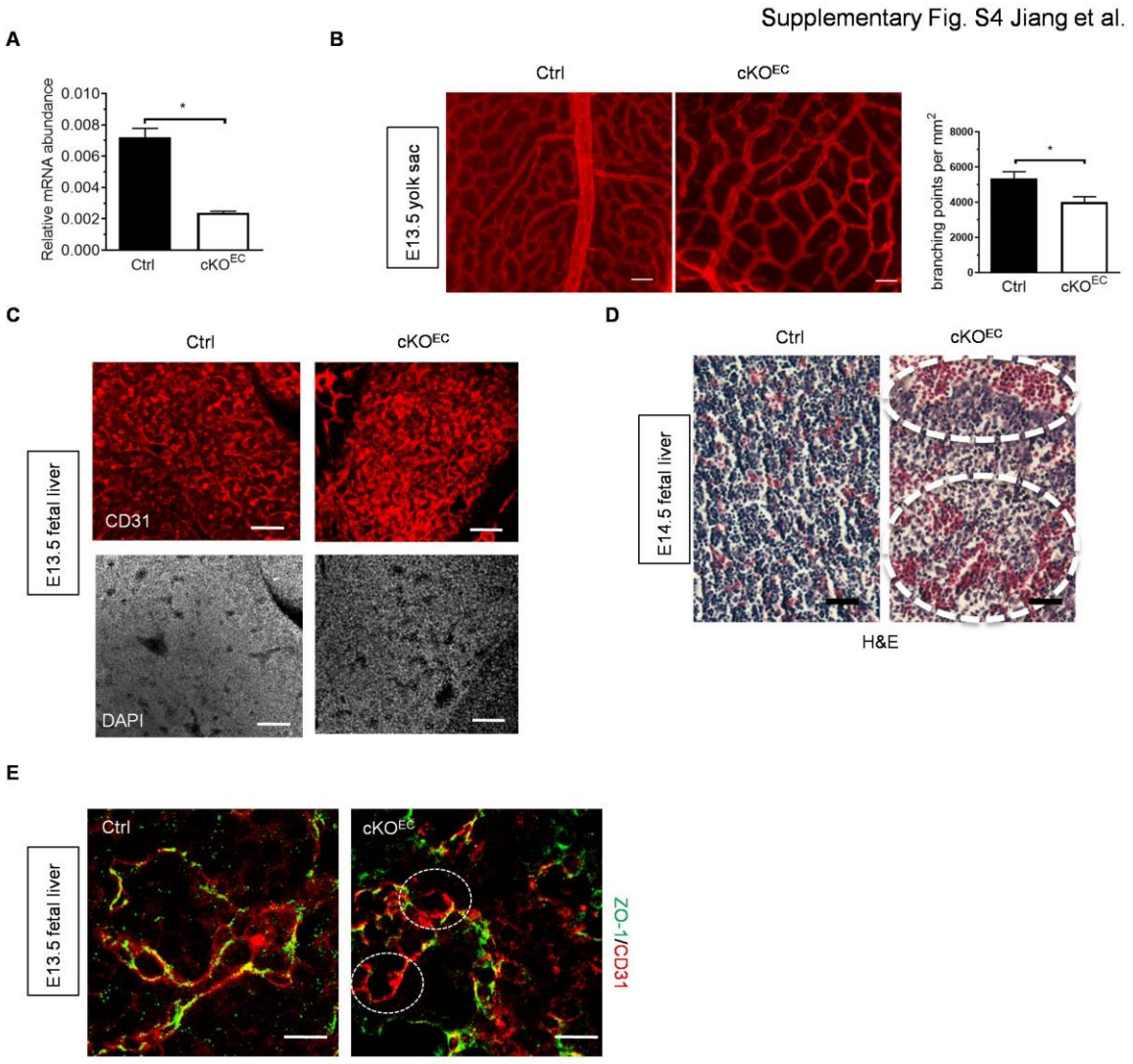

Fig. S4. *Drosha* cKO^{EC} embryos showed mild angiogenesis defects and a sign of hemorrhage. A. qRT-PCR analysis of *Drosha* mRNA abundance relative to GAPDH in endothelial cells (CD31^{+}CD45^{-}) sorted from E10.5 AGM is shown as Mean ±SEM . *P<0.05, significant by two tail unpaired Student t-Test. N=3 biological replicates. **B.** Representative images of whole mount immunofluorescence stain of CD31 in E13.5 yolk sac. Quantitative analysis of branching points are shown as Mean ±SEM (right). Scale bar: 100μm. N=4 Ctrl embryos and 3 cKO^{EC} embryos. *P<0.05, significant by two tail unpaired Student t-Test. **C.** Representative images of CD31 immunofluorescence of E13.5 fetal liver section. Scale bar: 100μm. N=3 Ctrl embryos and 3 cKO^{EC} embryos. **D**.H&E staining of E14.5 fetal liver sections from Ctrl or cKO embryos. White circles indicate the areas in which extravascular erythrocytes were detected. Scale bar: 100μm. N=4 embryos for each genotype. **E**. Representative immunofluorescence images of ZO-1 (green) and EC marker CD31 (red). White circles: the areas in which ZO-1 stain was disrupted. Scale bar : 20μm. N=3 Ctrl embryos and 3 cKO^{EC} embryos.

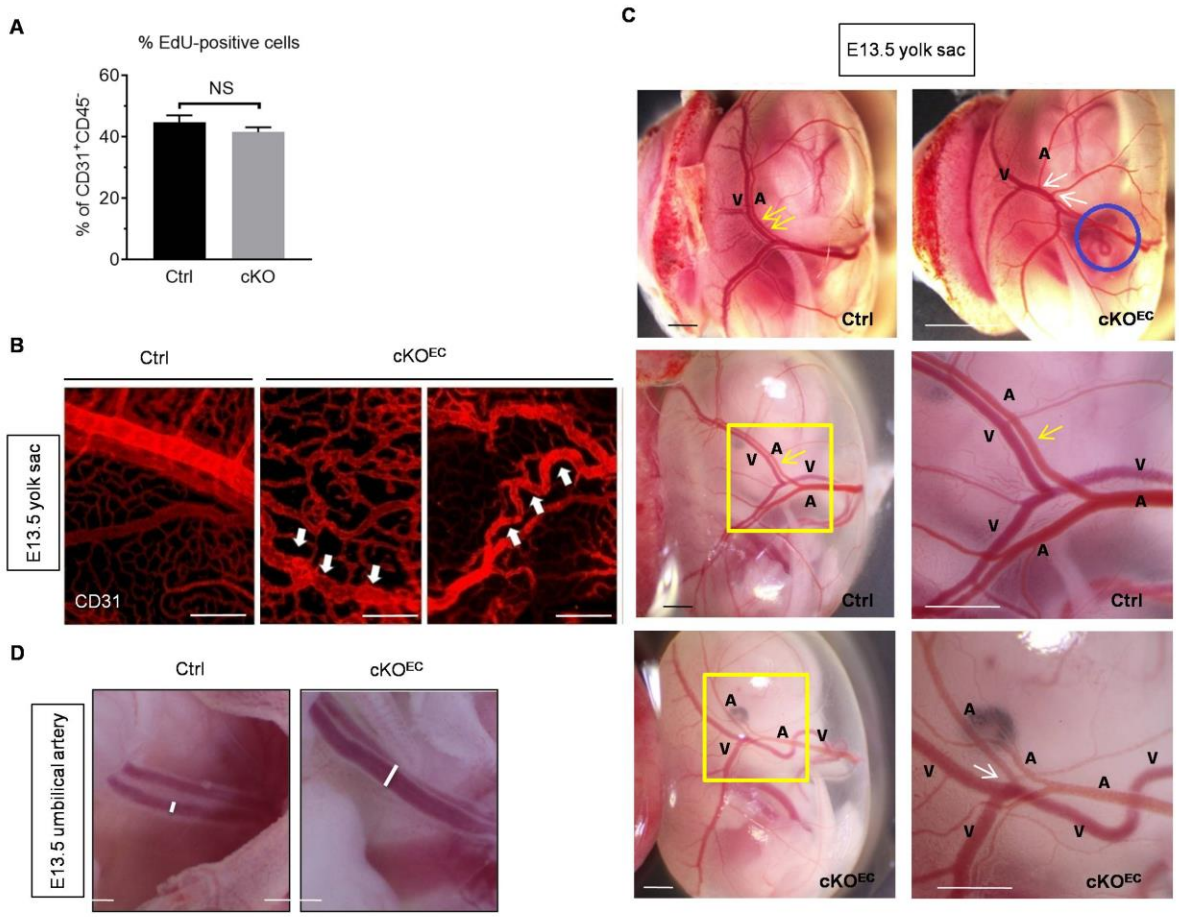

Fig. S5. ***Drosha*** **cKO^{EC} embryos showed disorganized and dilated vasculature. A.** The fraction (%) of proliferating cells among endothelial cells ($CD31^{+}CD45^{-}$ cells) from E10.5 Ctrl and cKO^{EC} embryo is shown as Mean ±SEM by counting EdU-positive cells by flow cytometry. N=3 cKO^{EC} embryos and 9 Ctrl embryos. NS, not significant by two tail unpaired Student t-Test. **B.** Representative images of whole mount CD31 immunofluorescence of E13.5 yolk sac vasculature. White arrow: tortuous vessels. Scale bar: 100μm. N=3 cKO^{EC} embryos and 6 Ctrl embryos. **C.** Representative images of E13.5 yolk sac vasculature. Blue circle, twisted vitelline vein. Yellow arrow, aligned artery and vein. White arrow, artery vein fistula. Regions of the yellow boxes were zoomed and shown in right. A, artery. V, vein. N= 10 cKO^{EC} embryos and 13 Ctrl embryos. Scale bar: 2mm. D. Representative images of extraembryonic vasculature. White bars indicate the diameter of umbilical artery (UA) in Ctrl and cKO^{EC} embryos. N= 5 cKO^{EC} embryos and 10 Ctrl embryos. Scale bar: 2mm.

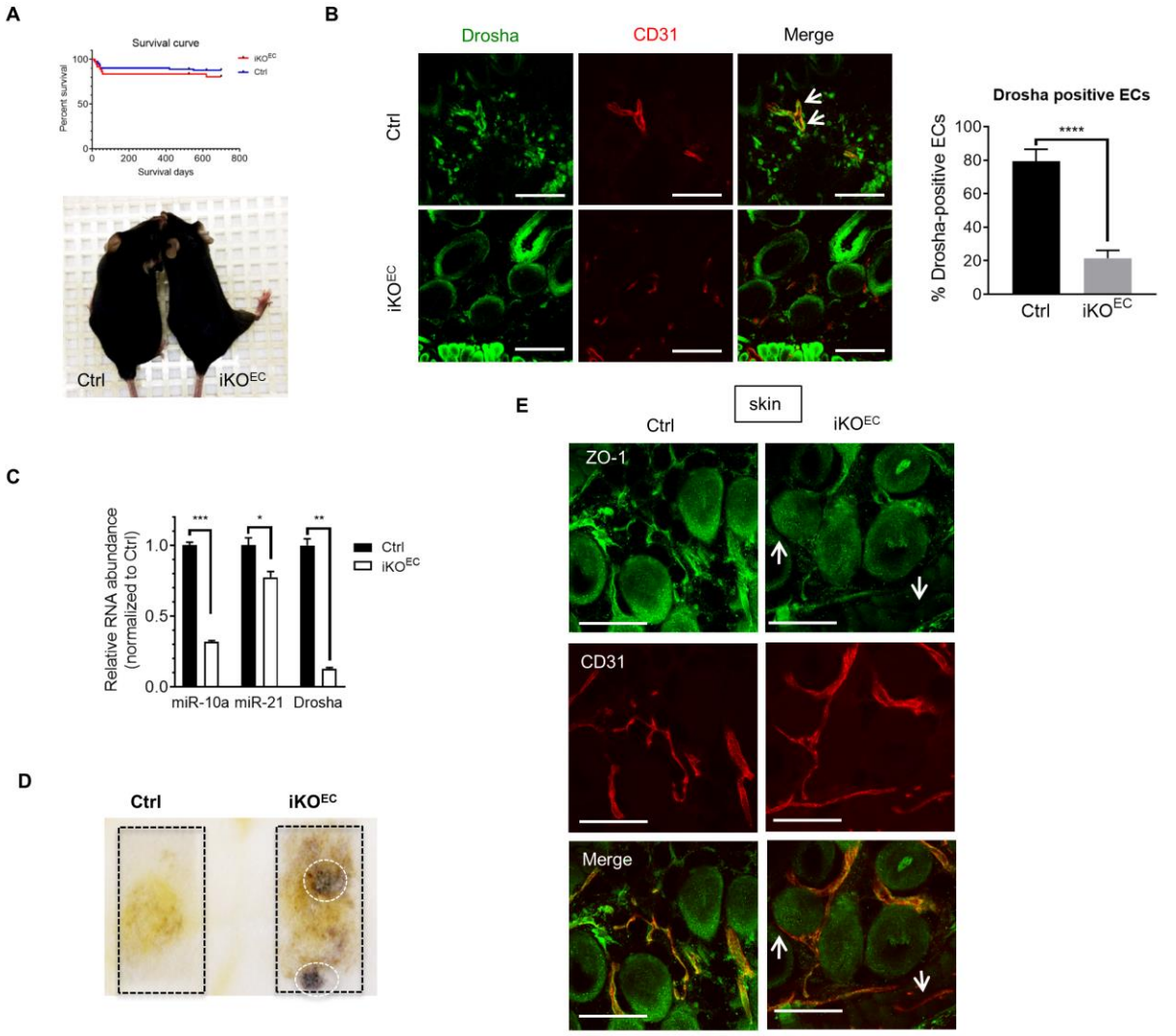

Fig. S6. *Drosha* iKO^{EC} mice show vascular leakage. A. Survival curve (top) and gross morphology (bottom) of 2-month-old iKO^{EC} or Control mice. Gehan-Breslow-Wilcoxon test was used to determine that Ctrl and iKO^{EC} survival curves are not significantly different. N=37 iKO^{EC} mice and 81 Ctrl mice. **B.** Representative immunofluorescence stain images of Drosha (green) and CD31(red). Quantitative analysis of the percentage of Drosha positive endothelial cells (ECs) among all the endothelial cells are shown as Mean ±SEM (right). ****P<0.0001, significant by two tail unpaired Student t-Test. White arrows indicate Drosha in the nucleus of endothelial cells in Ctrl mice. Scale bar: 100μm. N=3 for each genotype. **C.** Relative abundance of *Drosha* mRNA normalized to GAPDH and miRNA (miR-10a, -21) normalized to U6 snRNA in endothelial (CD31^{+}CD45^{-}) cells sorted from E18.5 liver of iKO^{EC} or Control embryos. RNA abundance was shown as Mean± SEM. *P<0.05, **P<0.01, ***P<0.001, significant by two tail unpaired Student t-Test. **D.** Feces from 8-month-old control or iKO^{EC} mice were subjected to the fecal occult blood test. Representative results are shown. Dark purple in circles: presence of hemoglobins. Yellow smear is the color of feces. Detection windows are indicated as the black boxes. N=3 mice for each genotype. **E.** Representative images of immunofluorescence staining for ZO-1 (green) and the endothelial cell marker CD31 (red) in the skin of 8 week old Ctrl or iKO^{EC} mice. White arrows indicate endothelial cells with reduced ZO-1 staining. N=3 mice for each genotype. Scale bar: 100μm.

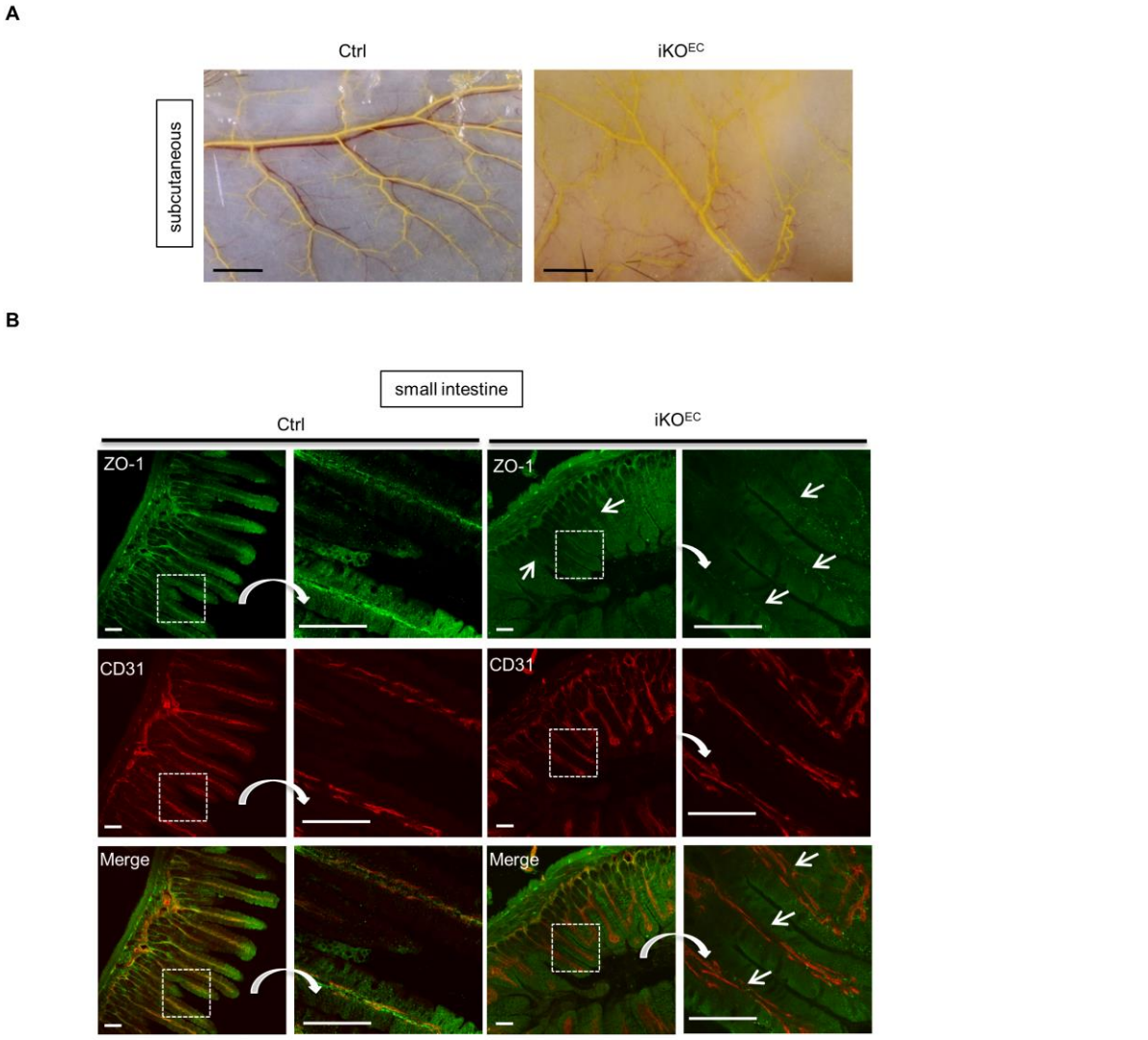

Fig. S7. The distribution of the tight junction protein ZO-1 is disrupted in the endothelial cells of *Drosha* iKO^{EC} mice. A. Representative images of the subcutaneous vasculature in the dorsal side of 8-month-old *Drosha* iKO^{EC} and Ctrl mice. Scale bar: 500μm. N=3 mice for each genotype. **B.** Representative images of immunofluorescence staining of ZO-1 (green) and the endothelial cell marker CD31 (red) of the small intestine of 13-months old Ctrl or iKO^{EC} mice. White arrows indicate endothelial cells with reduced ZO-1 staining. Scale bar: 100μm. N=3 mice for each genotype.

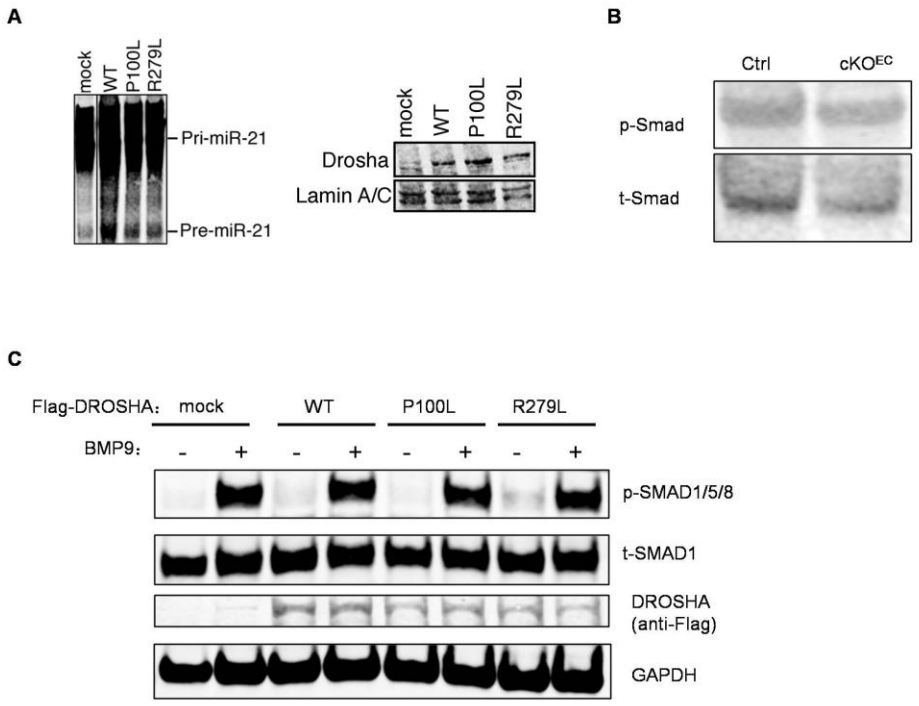

Fig. S8. In vitro processing assay of pri-miR-21 and the BMP-Smad signaling pathway in cells expressing DROSHA mutants or depleted of *Drosha*. A. In vitro-processing was performed with nuclear extracts from mouse embryonic fibroblasts (MEFs) exogenously expressing DROSHA WT, P100L, or R279L or that had been mock transfected. Immunoblot analysis of DROSHA and Lamin A/C (loading control) protein was performed (right) using nuclear extracts identical to the processing assay (top). Representative images are shown. N=3 independent experiments. **B.** Endothelial cells ($CD31^{+}CD45^{-}$) sorted from E13.5 fetal liver (N=4 mice per genotype analyzed as a pool) were combined and subjected to immunoblot analysis of phospho-Smad1/5/8 (p-Smad) and total Smad1(t-Smad). **C.** Immunoblot analysis of nuclear extracts of human microvascular endothelial cells (MVECs) in which DROSHA WT or mutants were exogenously expressed. MVECs were stimulated with or without 1 nM BMP9 for 2 hrs prior to preparation of cell lysates and immunoblot analysis. Anti-Flag, the antibody that recognize Flag tag. N=2 independent experiments.

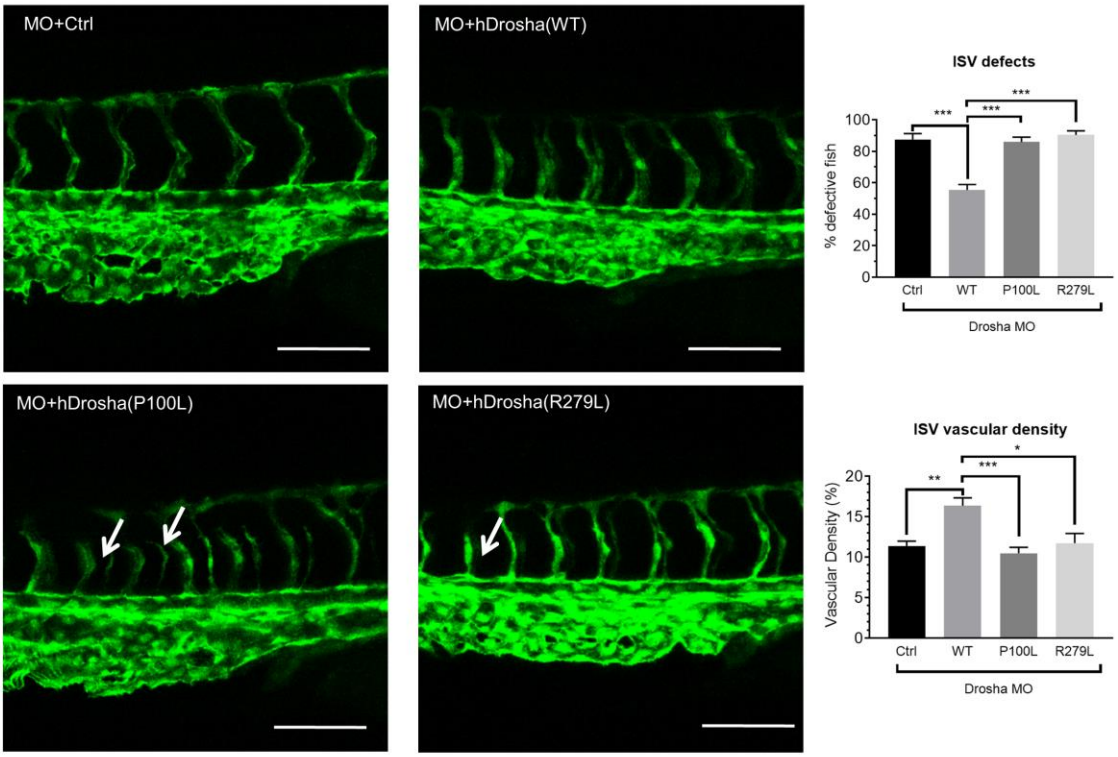

Fig. S9. ISV defects mediated by the knockdown of *Drosha* by morpholino oligos are rescued by coinjection of wild-type (WT) *Drosha* mRNA, but not by mutant mRNA. *Drosha* MO (1ng MO1+1ng MO2) and 100 pg T7 (Ctrl) RNA or human *Drosha* (*hDrosha*) WT or mutant mRNA were injected into *Tg(fli1:nEGFP)*^{y7}zebrafish at the 1-2 cell stage. Representative images of ISVs in the middle region of the fish are shown (left). Arrows indicate abnormal ISVs. Scale bar: 100 μM. The fraction (%) of fish with defective ISVs as indicated with arrows (right top panel) and vascular density (right bottom panel) are shown as Mean±SEM. n=97 zebrafish for Ctrl mRNA, n=88 zebrafish for hDrosha, n=91 zebrafish for hDrosha P100L mRNA, n=86 zebrafish for hDrosha R279L mRNA. *P<0.05, **P<0.01, ***P<0.001, significant by one-way ANOVA with post hoc Tukey's test.